Salt-stress-induced association of phosphatidylinositol-4,5-bisphosphate with clathrin-coated vesicles in plants

Sabine König, Till Ischebeck, Jennifer Lerche, Irene Stenzel, Ingo Heilmann

Salt-stress-induced association of phosphatidylinositol-4,5-bisphosphate with clathrin-coated vesicles in plants

Sabine König, Till Ischebeck, Jennifer Lerche, Irene Stenzel, and Ingo Heilmann

Affiliation (all):

Department of Plant Biochemistry
Albrecht-von-Haller-Institute for Plant Sciences
Georg-August-University Göttingen
Justus-von-Liebig-Weg 11
37077 Göttingen
Germany

Short title:
PtdIns(4,5)P_2 and vesicle formation

Corresponding author:
Ingo Heilmann
Department of Plant Biochemistry
Albrecht-von-Haller-Institute for Plant Sciences
Georg-August-University Göttingen
Justus-von-Liebig-Weg 11
37077 Göttingen
Germany
phone, +49 551 39-5748
fax, +49 551 39-5749
email iheilma@uni-goettingen.de

Key words:
Arabidopsis thaliana, PtdIns(4,5)P_2, clathrin-coated vesicles, hyperosmotic stress, lipids

Abbreviations:
AEBSF, 4-(2-aminoethyl)-benzolsulfonylfluoride; CCV, clathrin-coated vesicle; DAG, diacylglycerol; DAPI, 4',6-diamidino-2-phenylindol; DEDTC, diethyldithiocarbamate; DTT, dithiothreitol; EDTA, ethylenediamine tetraacetate; EGTA, ethyleneglycol tetraacetate; ER, endoplasmic reticulum; EYFP, enhanced yellow fluorescent protein; GC, gaschromatography; HFT, NFT, types of beam splitters; MBS, main beam splitter; $InsP_3$, inositol-1,4,5-trisphosphate; PLC, phospholipase C; PMSF, phenylmethylsulfonylfluoride; PtdCho, phosphatidylcholine; PtdEtn, phosphatidylethanolamine; PtdIns, phosphatidylinositol; PtdIns3P, phosphatidylinositol-3-phosphate; PtdIns4P, phosphatidylinositol-4-phosphate; PtdIns(4,5)P_2, phosphatidylinositol-4,5-bisphosphate; PVPP, polyvinylpolypyrrolidone; TLC, thin layer chromatography

Synopsis

Plants exposed to hyperosmotic stress undergo changes in membrane dynamics and lipid composition to maintain cellular integrity and avoid membrane leakage. Various plant species respond to hyperosmotic stress with transient increases in phosphatidylinositol-4,5-bisphosphate (PtdIns(4,5)P_2), however, the physiological role of such increases is unresolved. Here, the spatio-temporal dynamics of stress-induced changes in phosphoinositides (PIs) were analyzed in subcellular fractions of *Arabidopsis* leaves to delineate possible physiological roles. Unlabeled lipids were separated by thin-layer-chromatography and quantified according to gas-chromatographic detection of associated fatty acids. The plasma membrane represents the outermost barrier between the symplast of plant cells and its apoplastic surroundings. Transient PtdIns(4,5)P_2 increases upon hyperosmotic stress were detected first in enriched plasma membrane fractions, however, at later time points PtdIns(4,5)P_2 increased in endomembrane-fractions of the corresponding two-phase systems. When major endomembranes were enriched from rosette leaves prior to hyperosmotic stress and over 60 min of stimulation, no stress-induced increases in the levels of PtdIns(4,5)P_2 were found in fractions enriched for endoplasmic reticulum, nuclei, or plastidial membranes. Instead, increased PtdIns(4,5)P_2 contents were found in clathrin-coated vesicles (CCVs), which proliferated several-fold in mass within 60 min of hyperosmotic stress according to the abundance of CCV-associated proteins and lipids. Monitoring the subcellular distribution of fluorescence-tagged reporters for clathrin and PtdIns(4,5)P_2 during transient coexpression in onion epidermal cells indicates rapid stress-induced colocalization of clathrin with PtdIns(4,5)P_2 at the plasma membrane. The data indicate that PtdIns(4,5)P_2 may act in stress-induced formation of CCVs in plant cells, highlighting evolutionary conservation of the PI system between organismic kingdoms.

Introduction

Polyphosphoinositides (PIs) are central regulators of physiological processes in eukaryotic cells. Phosphatidylinositol-4,5-bisphosphate (PtdIns(4,5)P_2) has emerged as a multifunctional regulatory player in various biological model systems studied. By acting as a lipid ligand to various alternative protein partners PtdIns(4,5)P_2 can regulate localization or activity of specific target proteins, and ensuing effects on physiology in various eukaryotic organisms have been extensively reviewed [1-3]. Besides many other processes, vesicle trafficking in eukaryotic cells is influenced by PtdIns(4,5)P_2-protein interactions required for the assembly of the protein-machinery for vesicle fusion or -budding [4, 5] as well as by the particular biophysical properties of the inverse-conical lipid, exerting curvature strain on the membrane [6, 7]. Whereas the presence of PtdIns(4,5)P_2 in plants has been shown and changes in PtdIns(4,5)P_2 levels during various stress-responses have been reported [8-12], the particular adaptational processes regulated in plants by PtdIns(4,5)P_2 remain unclear, in part because the stress-activated lipid kinase(s) producing PIs remain unidentified. While increases in PtdIns(4,5)P_2 after hyperosmotic stress have been proposed to support increases is inositol-1,4,-trisphosphate (InsP_3) [9, 13], correlating with increases in cytosolic Ca^{2+} [12], no functional evidence has been provided linking these metabolite changes with the plant adaptational response. So far, it is not clear whether intact PtdIns(4,5)P_2, InsP_3, or other derived metabolites represent physiological stress-signals.

The subcellular distribution of PIs in a eukaryotic cell is a key factor in determining the regulatory effects that will be exerted by the lipids [14]. PIs and the activities of their biosynthetic enzymes have been found associated with different subcellular structures of plant cells [3, 15, 16], suggesting that different regulatory functions of PIs are exerted in different compartments. Previous work performed on plants provides evidence that PtdIns(4,5)P_2 and other PIs are organized in distinct lipid pools [8, 9, 13, 17] that may be independently regulated. The subcellular location of stress-induced increases of PtdIns(4,5)P_2 in plant cells may, thus, give important insights as to what physiological processes may be controlled by PtdIns(4,5)P_2.

In the present study, hyperosmotic stress was used as a well-characterized stimulus eliciting PtdIns(4,5)P_2 changes in plants [8, 9, 11, 12]. The exact physiological roles of stress-induced PtdIns(4,5)P_2 are unknown, however, functions will likely relate to stress adaptation. The most immediate threat posed by hyperosmotic stress are osmotic efflux of water and loss of turgor-pressure [18], leading to changes in cellular ultrastructure [19] and membrane leakage [20]. In order to maintain cellular integrity under hyperosmotic conditions, a number of membrane-rearrangement processes have been described from biological and artificial model systems that are thought to minimize membrane leakage [20]. A process immediately following osmotic water loss is bulk-flow endocytosis, by which excess membrane area is internalized into endomembrane vesicles to reduce the overall cell surface area and regain turgor pressure [18]. It has been suggested that the PI, PtdIns3P, is involved in endomembrane trafficking following bulk-flow endocytosis in plant cells [21]. While the PI system may, thus, be involved in plasma membrane-to-endomembrane trafficking in plants, a role for PtdIns(4,5)P_2 in related processes has so far not been demonstrated. Because it is known from other eukaryotic model systems that PtdIns(4,5)P_2 takes part in vesicle fusion or vesicle budding processes at the plasma membrane, for instance during synaptic exocytosis for neurotransmitter release and subsequent endocytotic membrane-recycling events [4, 5, 7], it was one working hypothesis of the present study that intact PtdIns(4,5)P_2 may have a role in the formation of endocytotic plasma membrane vesicles.

Here we show that PtdIns(4,5)P_2 formed upon hyperosmotic stress is associated first with enriched plasma membrane fractions of stressed *Arabidopsis* plants and is increased in the endomembrane fraction at later time points of stimulation. Increased PtdIns(4,5)P_2 levels are shown to associate with clathrin-coated vesicles (CCVs), whereas no increased levels of

PtdIns(4,5)P_2 are found in endoplasmic reticulum, nuclei, or plastidial membranes. Stress-induced colocalization of PtdIns(4,5)P_2 with clathrin is visualized in onion epidermal cells transiently coexpressing fluorescent reporters for PtdIns(4,5)P_2 and clathrin, suggesting a role for PtdIns(4,5)P_2 in the recruitment of coat-proteins to the plasma membrane during vesicle budding in plant cells.

Experimental

Plant growth conditions and stress treatments. All experiments were performed with *Arabidopsis thaliana* ecotype Columbia 0 (col-0). Plants were grown on soil under exposure to 140 µmol photons m^{-2} sec^{-1} of light in an 8 h light and 16 h dark regime. Seeds for plants destined for stress treatments were surface-sterilized for 5 min in 75 % ethanol, followed by 20 min incubation in 6 % (w/v) NaOCl in 0.1% (w/v) Triton X-100, washed 5 times in sterile distilled water. Seeds were vernalized at 4 °C for 2 d, followed by culture in sealed jars on 0.5% Murashige and Skoog medium including modified vitamins (Duchefa) containing 1% (w/w) sucrose and 0.25% (w/w) Gelrite (Roth). After 14 days plants were transferred to hydroponic cultures in liquid media as described [22]. Hydroponic cultures were exposed to 140 µmol photons m^{-2} sec^{-1} of light in an 8 h light and 16 h dark regime and continuously aerated. Eight to ten-week-old plants were treated by adding NaCl in final concentrations of 0.4 M and 0.8 M, respectively, to the hydroponic media. Rosette leaves were harvested before treatment and after various periods of stimulation, as indicated in the results section, and immediately frozen in liquid nitrogen. Care was taken to perform experiments over the same day-time period within the light-dark-regime, and not to cross the light-dark transition.

Enrichment of subcellular fractions

Plasma membrane and bulk endomembranes. Plant material (50-100 g) was snapfrozen in liquid N_2 and ground in the cold to a fine powder with mortar and pestle. The resulting powder was resuspended in cold 30 mM Tris-HCL, pH 7.4, containing 200 mM sucrose, 14 mM b-mercaptoethanol, 2 mM dithiothreitol, 3 mM EDTA, 3 mM EGTA, 1 mM PMSF, 1.5 % (w/v) PVPP, and 10 µg ml^{-1} Leupeptin and subjected to 20 movements in a glas douncer on ice. The resulting extract was cleared by centrifugation for 15 min at 3700 x g at 4°C. The supernatant was centrifuged for 45 min at 25500 x g at 4°C to pellet total cellular membranes. The total membrane pellet was used for plasma membrane preparation by aqueous two-phase-partitioning on 6.3 % (w/w) mer gradients as previously described [10].

Endoplasmic reticulum. Plant material (50-100 g) was macerated with a razor blade and resuspended in 1 ml g^{-1} of cold buffer A (40 mM Hepes, pH 7.5, containing 400 mM sucrose, 10 mM KCl, 3 mM $MgCl_2$, 1 mM DTT, and 0.1 mM EDTA). The homogenate was filtered through one lyer of miracloth and cleared by centrifugation for 20 min at 6000 x g at 4°C. From the supernatant ER-membranes were enriched as previously described [23].

Nuclei. Plant material (50-100 g) was snapfrozen in liquid N_2 and ground in the cold to a fine powder with mortar and pestle. The resulting powder was resuspended in 1 ml g^{-1} of cold buffer B (25 mM Mes-KOH, pH 6.2, 5.5 M glycerol, 600 mM sorbitol, 10 mM β-mercaptoethanol, 5 mM EDTA, 0.5 mM DEDTC, 0.5 mM AEBSF, 0.5 mM spermidine, 0.2 mM spermine, 0.05 % (w/v) Triton x-100, 0.1 mg ml^{-1} delipidated BSA (Sigma), and 0.1 mg ml^{-1} PVP-40) and incubated for 30 s. The suspension was sequentially filtered through Nylon-meshes of decreasing pore size (250 µm, 80 µm, 20 µm). The filtrate was collected and used for the enrichment of nuclei using percoll gradients as previously described [24].

F-actin. Plant material (50-100 g) was snapfrozen in liquid N_2 and ground in the cold to a fine powder with mortar and pestle. The powder was resuspended in 1 ml g^{-1} of cold 5 mM Hepes-KOH, pH 7.5, containing 10 mM Mg-acetate, 2 mM EGTA, 1 mM PMSF, and 0.5 % (w/v) PTE and used for enrichment of of filamentous actin as previously described [25].

Plastids. Plant material (50 g) were homogenized for 3 x 5 s using a polytron homogenizer (PCU-2, Typ 10203500, Kinematic, Luzern, CH) in 50 ml cold 20 mM HEPES/KOH, pH 8.0, containing 0.3 M sorbitol, 5 mM $MgCl_2$, 5 mM EGTA, 5 mM EDTA, 10 mM $NaHCO_3$ in a 150-ml beaker. The homogenate was filtered through a double layer of Miracloth. The debris retained in the Miracloth was returned to the beaker with 20 ml fresh isolation buffer and the homogenisation was repeated. Plastid enrichment was carried out on the filtrate as previously described [24].
Clathrin-coated vesicles. Plant material (50-100 g) was homogenized in 1 ml g^{-1} of cold buffer A using a polytron homogenizer (PCU-2, Typ 10203500, Kinematic, Luzern, CH). The homogenate was filtered through three layers of miracloth and was cleared by centrifugation for 50 min at 8000 x g at 4°C. CCVs were enriched as previously described [24].
The lipid phosphatase inhibitor (3S)[1,1-difluoro-3,4-bis(oleoyloxy)butyl] phosphonate (Echelon) was included in all buffers at a final concentration of 3 µM.

Marker tests. Biochemical tests for enrichment of particular subcellular fractions were performed as previously described: concanavalin A binding [26]; β1,3-glucan synthetase and NADH cytochrome C reductase [27]; DAPI-staining [28]; chlorophyll estimation [29].

Protein electrophoresis and immunodetection. Protein contents were determined according to the Bradford method [30], using BSA as a standard. Proteins were separated by SDS-PAGE analysis as previously described [31] using the Mini-Protean 3-System (Biorad). Proteins were transferred from acrylamide gels onto nitrocellulose membranes (Roti-Nylon 0.2 Transfermembran, 0.2 µm; Roth) using the wet-blot system Mini-Protean 3 (Biorad). Membranes were washed and blocked as previously described [8]. Immunodetection was peerformed using the following antisera: rabbit anti-PMA2 [32]; rabbit anti-actin (Sigma); rabbit anti-TGA2 (provided by Dr. C. Gatz, Göttingen); rabbit anti-BiP [33]; mouse anti-clathrin (Sigma, [34]), and rabbit anti-V-ATPase [35]. Primary antisera were detected using appropriate secondary antisera (Sigma) conjugated to alkaline phosphatase. Alkaline phosphatase was detected using a color reagent (Sigma) containing nitroblue tetrazolium chloride and 5-bromo-4-chloro-3'-indolyphosphate p-toluidine, as previously described [36].

Lipid extraction and biochemical analyses. PIs were extracted using an acidic extraction protocol [37]. Lipids were separated by thin-layer-chromatography (TLC) on silica gel plates (Merck) using developing solvents for optimal resolution: for PIs, $CHCl_3$:CH_3OH:NH_4OH:H_2O (57:50:4:11(v/v/v/v)) [38]; for PtdCho and PtdEtn, acetone:toluol:water (91:30:7 (v/v/v)) [39]; for isolating phosphatidylinositol, $CHCl_3$:methyl acetate:isopropanol:CH_3OH:0.25% aqueous potassium chloride (25:25:25:10:9 (v/v/v/v/v)) [40]. Lipids were isolated and analyzed for associated fatty acids as previously described [41]. Variation in fatty acid patterns obtained with material sampled on different days did not exceed that denoted by standard deviations. Due to limiting material in samples representing isolated minor lipids, fatty acids of low abundance may be absent from fatty acid patterns.

cDNA constructs. cDNA fragments for EYFP (Clontech) and RedStar [42] were amplified from plasmids carrying the authentic clones provided by Dr. Martin Fulda (Göttingen University, Germany) using the following primer combinations: EYFP, 5'-GATCGCGGCCGCCCATGGTGAGCAAGGGCGAG-3'/5'-GATCGATATCTTACTTGTACAGCTCGTCCATG-3'; RedStar, 5'-GATCGTCGACATGAGTGCTTCTTCTGAAGATGTC-3'/5'-GATCGCGGCCGCCAAGAACAAGTGGTGTCTACCTT-3'. The coding sequence for the human PLCδ1-PH-domain was amplified from plasmid-DNA provided by Dr. Tamas Balla [43] and modified to encode a seven-amino acid linker (gly-gly-ala-gly-ala-ala-gly) between

the PH domain and the RedStar as previously described [44], using the primer combination 5'-GATCGCGGCCGCCGGTGGAGCTGGAGCTGCAGGAATGAGGATCTACAGGCGC -3'/5'-GATCGATATCTTAGATCTTGTGCAGCCCCAGCA-3'. The coding sequence for the *Arabidopsis* clathrin light chain was amplified from *Arabidopsis* leaf cDNA using the primer combination 5'-GATCGCGGCCGCCATGGGCTCTGCCTTTGAAGACGATTCCTTC-3'/5'-GATCGCGGCCGC TTAAGCAGCAGTAACTGCCTCAGT-3'. cDNA sequences encoding fluorescence tags were subcloned into *pGemTeasy* and moved into *pUC18Entr* [45] as a *Not*I/*Eco*RV-fragment (EYFP) or as a *Sal*I/*Not*I-fragment (RedStar), creating the plasmids *pUC18Entr-EYFP* and *p18Entr-RedStar*, respectively. Prior to ligation, the *ccdb* gene was eliminated from *pUC18Entr* by *Eco*RI digestion and religation. The cDNA sequence encoding clathrin was moved into pUC18Entr-EYFP as a NotI/NotI-fragment; that encoding PLCδ1-PH into *pUC18Entr-RedStar* as a *Not*I/*Eco*RV-fragment. Inserts in the resulting plasmids were transferred to the plasmid *pCAMBIA3300* [45] by using Gateway technology (Invitrogen) according to the manufacturer's instructions.

Detection of specific transcripts by RNA-DNA hybridization. RNA was extracted from rosette leaves of hydroponically grown plants at different time points after exposure to salt treatment as previously described [46]. cDNA probes were amplified from whole *Arabidopsis* cDNA using the primer combinations 5'-GTCTTCTTCTTCTACATAAAATTG-3'/5'-GGAAATTATTAGCGTTGTCATTA-3' (HVA) or 5'-AATGTGTACGTCTTTTGCATAAG-3'/5'-GTAACATCTTCTCTTATTTATATAA-3' (RD20) and radiolabeled by random priming. Hybridizations were performed as previously described [13].

Particle bombardment and transient expression in onion cells. Transient gene expession in onion epidermal cells was achieved by ballistic bombardment of plant material with DNA-coated gold-particles [47]. Five µg of plasmid DNA were precipitated onto gold particles (1.0 mm, Biorad, Hercules, CA, USA). Fresh onions (*Allium cepa L.*) were cut and the pieces were placed on wet filter paper. Whole pieces were bombarded with a Biolistic PDS 1000/He Biolistic Particle Delivery System (Biorad) with 1350 psi rupture discs under a vacuum of 0.1 bar. After bombardment samples were incubated at high humidity for 24 h. Onion skin epidermal cell layers were peeled and transferred to glass slides for microscopic examination. Stress-treatments were applied directly on microscope slides by adding 0.2 M NaCl in culture medium and drawing the solution under the cover slip.

Confocal imaging. Images were recorded using a Zeiss LSM 510 confocal microscope. EYFP was excited at 514 nm and imaged using an HFT 405/514/633 nm major beam splitter (MBS) and a 530-600 nm band pass filter; RedStar was excited at 561 nm and imaged using an HFT 405/488/561 nm MBS and a 583-604 nm band pass filter. In coexpression experiments, EYFP and RedStar were synchronously excited at 488 nm and 561 nm, respectively, and imaged using an HFT 405/488/561 nm MBS and a 518-550 nm band pass filter and a 583-636 nm band pass filer, respectively. Images were obtained by confocal microscopy at 1000 x magnification using the Zeiss LSM510 image aqcuisition system and software (v 4.0, Zeiss). Fluorescence and transmitted light images were contrast-enhanced by adjusting brightness and γ-settings using image-processing software (Photoshop; Adobe Systems).

Results

In order to delineate a physiological function for PtdIns(4,5)P_2 formed upon hyperosmotic stress in *Arabidopsis* leaves, a direct approach of subcellular fractionation

combined with lipid analysis was chosen to systematically test various subcellular compartments for increased PtdIns(4,5)P_2 levels after stress application.

Characterization of organellar fractions enriched from *Arabidopsis* rosette leaves

In order to delineate the subcellular sites of PtdIns(4,5)P_2, in a first step different subcellular fractions were enriched from *Arabidopsis* rosette leaves. Enriched subcellular fractions included the plasma membrane, an F-actin cytoskeletal fraction, ER, nuclei, plastids and CCVs. When lipid patterns associated with the enriched fractions were analyzed (Fig. 1), neutral lipids and the plastidial galactolipids, monogalactosyldiacylglycerol and digalactosyldiacylglycerol, were reduced in fractions enriched for ER, plasma membrane, F-actin, or CCVs in comparison to total microsomal preparations. In contrast, the nuclear preparation still contained plastidial galactolipids. The F-actin-enriched fraction contained only small amounts of membrane lipids, whereas substantial amounts of PtdEtn were detected in ER-enriched fractions. The CCV-enriched fractions were pooled from five independent preparations because of limited material and may contain additional ribosomal contaminations [48]. As a prerequisite for all further investigations, fractions were analyzed for cross-contamination of marker proteins using immunodetection (Fig. S1). Antisera used for immunodetection were against the plasma membrane ATPase PMA2 [32], actin, the nuclear transcription factor TGA2 [49], the ER-luminal binding protein BiP [33], clathrin [34], and the microsomal V-ATPase [35]. When enriched fractions were individually tested against all antisera, the resulting detection patterns indicated substantial enrichment of all fractions with only minor cross-contamination between the compartments tested. Because of limiting material the CCV-enriched fraction was not tested for actin (indicated by the x). The V-ATPase was detected in all fractions, as expected from its broad distribution and possibly indicating contamination of all fractions with other endomembranes than those specifically tested for. Enriched fractions were additionally subjected to a variety of marker tests as previously described [26-29], indicating substantial enrichment from the crude extracts (Fig. S2). Note, that the fractions used are not pure and represent only an enrichment from total microsomal pellets. Enriched subcellular fractions used in subsequent experiments were prepared as the fractions shown in Figure 1 and were additionally subjected to PI analysis.

Fatty acids associated with phospholipids do not differ between most organellar fractions in non-stimulated plants

In order to test whether direct detection of unlabeled lipids by the method outlined by [41] is sufficiently sensitive to detect even minor lipid constituents in plant lipid extracts, phospholipids were isolated from the various preparations and analyzed as previously described [41] (Fig. 2). The results indicated that non-labeled PIs can be detected in complex plant lipid extracts. Note that the exogenous PtdIns(4,5)P_2 was added to the extract in sample II at a concentration not detectable by charring (Fig. 2 A). The exogenous PtdIns(4,5)P_2 contained arachidonic acid, a fatty acid not endogenously present in *Arabidopsis*, and this fatty acid was detected by subsequent GC analysis of PtdIns(4,5)P_2 isolated from sample II (Fig. 2 B).

We have previously reported association of mainly saturated and monounsaturated fatty acids with bulk PIs isolated from non-stimulated *Arabidopsis* rosette leaves in contrast to a more unsaturated fatty acid composition in structural phospholipids, such as PtdCho or PtdEtn [9]. Structural phospholipids and PIs from the enriched subcellular fractions were analyzed for their associated fatty acids (Fig. 3) to identify subcellular compartments containing unsaturated PtdIns along with saturated or monounsaturated PIs, indicative of candidate locations for stress-induced PI function. The comparison of the fatty acid patterns of PIs, PtdIns4P and PtdIns(4,5)P_2 with those of structural phospholipids, PtdEtn, PtdCho and PtdIns (Fig. 3), confirmed increased association of saturated or monounsaturated fatty acids

with PIs in all fractions except in nuclei. In contrast, structural phospholipids contained higher proportions of unsaturated fatty acids. While fatty acid patterns for a given lipid were overall similar between enriched subcellular fractions, the fatty acid patterns observed for phospholipids isolated from nuclear extracts differed from the other extracts in containing an unusual combination of palmitic and oleic acids in structural phospholipids and PtdIns4P and an increased proportion of linoleic acid associated with PtdIns(4,5)P_2. While the distinct fatty acid pattern for nuclear lipids supports successful enrichment of nuclei (cf. Fig. 1), the physiological relevance of the fatty acid composition of nuclear lipids in plants is not clear. While some recent reports from the mammalian field indicate distinct roles for nuclear PIs [50, 51], in the course of this study no further experiments were performed to elucidate the particulars of nuclear phospholipids. With the noted exception, the data indicate that PIs associated with major subcellular fractions do not exhibit characteristic fatty acids patterns that could serve as a means for easy functional distinction and demonstrate that precursors of PtdIns(4,5)P_2-production can be found in all compartments tested.

Transient increases of PtdIns(4,5)P_2 in the plasma membrane are followed by increased PtdIns(4,5)P_2 levels in endomembranes

Because the analysis of different subcellular fractions did not suggest a particular compartment as the site for stress-induced PtdIns(4,5)P_2 formation, subcellular fractions enriched from plants subjected to hyperosmotic stress were systematically tested for increases in PtdIns(4,5)P_2. Because the plasma membrane represents the immediate barrier between the symplast and its apoplastic surroundings, the first fraction tested was that enriched for plasma membranes (Fig. 4, top panels). A transient increase in PtdIns(4,5)P_2 was evident after 15 min of stress application, which was followed by a decrease in plasma membrane PtdIns(4,5)P_2 at later time points. Plasma membrane enrichment by aqueous two-phase-partitioning yields a corresponding phase containing the residual endomembranes for each sample. PtdIns(4,5)P_2 levels in these residual endomembrane fractions indicate a gradual increase in PtdIns(4,5)P_2 in endomembranes at time points beyond 15 min of stimulation (Fig. 4, bottom panels). While plasma membrane PtdIns4P showed a similar dynamic pattern as plasma membrane PtdIns(4,5)P_2, PtdIns4P decreased first in endomembranes and showed increased levels only after 60 min of stimulation (Fig. 4); PtdIns-levels increased gradually with stimulation in both the plasma membrane and in endomembranes (Fig. 4).The data indicate that hyperosmotic stress-induced PtdIns(4,5)P_2 is generated first in the plasma membrane and can be found in endomembranes at later time points.

Stress-induced PtdIns(4,5)P_2-increases are excluded from ER, nuclei, or plastidial membranes

To define the endomembrane location at which PtdIns(4,5)P_2 increased at later time points, subcellular fractions enriched for major endomembrane systems of leaf tissue were prepared at different time points of stimulation, namely for ER, nuclei or plastids, and the fractions were analyzed for the levels of associated PIs, including PtdIns(4,5)P_2 (Figure 5). In the ER, nuclei or plastids detectable levels of PtdIns(4,5)P_2 were present (Fig. 5), however, no increase in the levels determined was observed correlated with application of the stress. PI levels associated with plastids were substantially lower than those detected in ER or nuclei, indicating little cross-contamination of samples. Overall, the dynamics of the lipids investigated indicate that the three major endomembrane systems tested did not contribute to stress-induced increases in cellular PtdIns(4,5)P_2 levels.

Decreasing PI levels in endomembrane fractions are not related to irreversible tissue damage

The failure to detect stress-induced increases in PtdIns(4,5)P_2 in the major endomembranes despite of extensive experimental efforts raised the question whether or not the plants were irreversibly damaged by the severe hyperosmotic stress applied. In order to rule out that decreasing lipid levels in endomembrane fractions observed were a consequence of irreversible loss of structural integrity, plants were subjected to hyperosmotic stress and tested for increases in stress-inducible transcript levels over a period of 24 h by Northern-blot experiments (Fig. 6). The stress-inducible transcripts for the genes HVA22 [52] and RD20 [53] showed substantial increases after 4-8 h and from 1 to 24 h, respectively, indicating that the induction of stress-inducible transcripts occurred as expected for non-damaged plants. Irreversible damage can, thus, be ruled out as a cause for the lipid patterns observed. Note that lipid patterns are reported for a period of only one h, whereas changes in transcript levels and plant survival were observed up to 24 h.

Hypertonic stress induces increased formation of CCVs in *Arabidopsis* leaves

Because the investigation of major endomembrane compartments (Fig. 5) had not revealed the location of the stress-induced increase in PtdIns(4,5)P_2, minor endomembrane compartments were also considered. A minor endomembrane fraction with relevance to physiological adaptation to hyperosmotic stress are CCVs. CCVs were isolated from *Arabidopsis* leaves prior to stimulation and after 60 min of hyperosmotic stress (Fig. 7). CCV-associated proteins from several preparations representing 30 g of leaf fresh weight were pooled and subjected to SDS-PAGE (Fig. 6 A). In-gel quantification of protein staining intensities indicates a stress-induced >2-fold increase in CCV-associated proteins within 60 min of stimulation (Fig. 7 A). Phospholipids were extracted from the same material and quantified (Fig. 7 B). The raised levels of the structural phospholipids, PtdEtn and PtdCho, also indicate an increase in CCV mass within 60 min of stimulation, supporting a role for CCV-formation in plant stress adaptation to hypertonic conditions.

Association of stress-induced PtdIns(4,5)P_2 with enriched clathrin-coated vesicles

CCVs enriched from plants exposed to hypertonic stress for different time periods were analyzed for PI content (Fig. 8). Within 30 min of hyperosmotic stress, the levels of CCV-associated PtdIns increased several fold, and after 60 min dramatic increases also in PtdIns4P and PtdIns(4,5)P_2 were observed. While the stress-induced CCV-associated PtdIns and PtdIns4P contained a large proportion of the unsaturated fatty acids, linoleic and linolenic acids, the increased PtdIns(4,5)P_2 was increased in stearic acid and oleic acid in addition to an increased proportion of linolenic acid (Fig. 8 A). The data identify CCVs as one of the endomembrane compartments harboring the stress-induced increase in PIs and PtdIns(4,5)P_2. The mass ratio of PtdIns(4,5)P_2/PtdCho was calculated (Fig. 8 B) and indicates that increased PtdIns(4,5)P_2 levels in CCVs were not merely a reflection of increased CCV mass (cf. Fig. 7), but rather a true increase in the proportion of CCV-associated PtdIns(4,5)P_2.

Stress-induced colocalization of PtdIns(4,5)P_2 with clathrin at the plasma membrane

In order to verify the biochemical findings of CCV-associated PtdIns(4,5)P_2 by an independent method, fluorescence-tagged markers for clathrin and for PtdIns(4,5)P_2 were transiently coexpressed in onion epidermal cells, the cells subjected to hyperosmotic stress, and the fluorescence distribution over time monitored by confocal microscopy (Fig. 9). The clathrin reporter construct encoded a fusion protein of clathrin with a C-terminally attached EYFP-tag; the PtdIns(4,5)P_2-reporter construct encoded the PH-domain of the human PLCδ1, which specifically binds to PtdIns(4,5)P_2, fused to a C-terminal RedStar-tag [42]. Prior to stimulation the clathrin reporter was distributed evenly throughout the cytosol, whereas the PtdIns(4,5)P_2-reporter was located at the plasma membrane (Fig. 9). When cells were subjected to hyperosmotic stress, within 2 min the clathrin reporter relocalized to the plasma

membrane to show a distribution now identical to that of the PtdIns(4,5)P_2-reporter. As hypertonic plasmolysis set in at later time points and endocytotic vesicles are too small to be reliably identified in cells undergoing dramatic structural reorganization, no time points later than 2 min were evaluated with confidence. Structural rearrangements of the plasma membrane were seen as early as 60 s after stress-application, evident by the rough appearance and multiple membrane invaginations (Fig. 10). The observed pattern of fluorescence distributions indicates rapid stress-induced relocalization of clathrin to sites containing PtdIns(4,5)P_2, thus corroborating the biochemical data.

Discussion

Direct detection of unlabeled PIs was employed to determine the subcellular location of transient increases in PtdIns(4,5)P_2 during hyperosmotic stress in *Arabidopsis* rosette leaves. The direct detection of PIs provides substantial advantages over approaches using radiolabeling because it is possible to quantify total lipid mass changes in comparison with changes in relative radiolabel incorporation, which is additionally subject to a number of factors, such as uptake and metabolic state of the labelled tissues, that are difficult to control for. It was the rationale of this study that the subcellular sites of PI changes upon stress may suggest physiological functions of the increased lipid levels.

Classical techniques for subcellular fractionation were used to enrich plasma membranes and various endomembrane fractions, and it is clear that the quality of the analyses shown depends on the quality of enrichment. The lipid patterns characteristic for individual subcellular fractions as well as the immunodetection of marker proteins and enzyme tests indicate substantial enrichment of the respective fractions (Figs. 1, S1 and S2). It must be noted that fractions obtained by the methods used will no doubt contain elements of other subcellular compartments than those enriched for. Importantly, however, the immunodetection of marker proteins indicates little cross-contamination between the enriched fractions tested (Fig. S1), which represent some of the major pools reported to contain PIs in eukaryotic cells. While contamination by other compartments cannot be ruled out, the effects of, for instance, mitochondrial membranes on PI patterns will be small.

When phospholipids were extracted from enriched subcellular fractions and analyzed for amount and nature of their associated fatty acids, structural phospholipids and PtdIns contained high proportions of unsaturated fatty acids, in particular linoleic and linolenic acids (Fig. 3), as was previously reported for extracts from whole cells [9]. In contrast, PIs, PtdIns4P and PtdIns(4,5)P_2, isolated from these enriched subcellular fractions contained close to no unsaturated fatty acids, as was also previously reported for whole cell extracts [9]. These data indicate that there may be no organelle-specific "fatty acid signature" of phospholipids or PIs. An exception is presented by nuclear extracts, which showed marked differences in the fatty acid compositions of all phospholipids in comparison to extracts from other enriched fractions (Fig. 3). While lipid patterns (Fig. 1) were ambiguous with respect to the purity of the nuclear extracts, the distinct fatty acid pattern of the nuclear lipids (Fig. 3) indicates a substantial degree of enrichment. The distinct fatty acid patterns of nuclear lipids, especially those of PIs, may prove relevant in the future possibly in support of recent reports of independent functions for nuclear PIs [50, 51]. Nuclear lipid patterns were, however, not a focus of this study, and because no stress-induced increases in PtdIns(4,5)P_2 were associated with nuclei (Fig. 5) these results shall not be further discussed at this point. Overall the fatty acid patterns for various phospholipids and PIs from enriched subcellular fractions of non-stimulated *Arabidopsis* leaves (Fig. 3) confirmed that various subcellular compartments contain the elements required for PtdIns(4,5)P_2-production, and, thus, the question for the subcellular sited of stress-induced PtdIns(4,5)P_2 -formation remained open.

By using direct detection of unlabeled lipids, subsequently a transient increase in PtdIns4P and PtdIns(4,5)P_2 could be located in enriched plasma membranes (Fig. 4). Early

increases in plasma membrane PIs with hypertonic stress may be related to the fact that the plasma membrane is the primary site of contact of the cell with its apoplastic surroundings. The transient nature of the plasma membrane PtdIns(4,5)P_2 increase and the subsequent increase in endomembranes (Fig. 4) may reflect lipid relocation either underlying or in consequence of dynamic membrane rearrangements to maintain cellular integrity during conditions of hyperosmotic stress. From the data presented it remains unclear whether PIs formed at the plasma membrane are internalized into endomembranes or whether the endomembranes hold stress-activated enzymes for PI biosynthesis. Although to our knowledge no stress-activated isoforms of PI kinases have been reported to date, it appears relevant in this context that the *Arabidopsis* PI4P 5-kinase isoform 1 heterologously expressed in tobacco BY2-cells relocated from the plasma membrane to endomembranes when the cells were exposed to hyperosmotic stress [54].

While previous reports have demonstrated association of PIs with ER [55, 56], nuclei [50, 51] and plastid envelope membranes [57, 58], the systematic analysis of the different endomembrane fractions revealed that the increased PtdIns4P and PtdIns(4,5)P_2 levels observed in total endomembranes were not associated with these locations (Fig. 5). A stress-induced increase in PtdIns (Fig. 5) was found only in fractions enriched for ER, an observation consistent with ER-associated PtdIns-biosynthesis reported previously [59-61]. The data suggest that PI pools present in ER, nuclei or plastids are not sensitive to hypertonic stress. Increased contents of PtdIns4P and PtdIns(4,5)P_2 with stress were positively identified in fractions enriched in CCVs (Fig. 8), which are formed at the plasma membrane in a stress-inducible manner (Fig. 7). The fatty acid composition of the CCV-associated PIs was highly unsaturated (Fig. 8) compared to that of PIs that were constitutively present in *Arabidopsis* (Fig. 3). This observation appears relevant in context of a recent report suggesting that PtdIns(4,5)P_2 containing long-chaing polyunsaturated fatty acids may be required for synaptic vesicle endocytosis in *Caenorhabditis elegans* [62]. While in the present study a protocol for vesicle enrichment was chosen that yielded a vesicle fraction defined by an easily detectable marker (clathrin), vesicle association of PtdIns(4,5)P_2 may not be limited to CCVs and the lipid may also associate with other types of vesicles. While the direct biochemical detection of PtdIns4P and PtdIns(4,5)P_2 associated with CCVs to our knowledge has not been reported before, it has been demonstrated for mammalian cells that clathrin, the major coat protein of CCVs, is recruited to CCVs in a PtdIns(4,5)P_2-dependent fashion [63]. The observation that PtdIns(4,5)P_2 increases first at the plasma membrane and subsequently in CCVs (Figs. 4 and 8) is corroborated by microscopy data (Fig. 9), indicating a rapid stress-induced relocation of clathrin from the cytosol to the plasma membrane. In a previous study it was shown that the PLCδ1-PH-reporter for PtdIns(4,5)P_2 is found in the cytosol of non-stimulated cells and will relocate to the plasma membrane upon hyperosmotic stress [64]. Our observation of plasma membrane association of the reporter may indicate that our "non-stimulated" cells were already in a stimulated state, possibly due to handling and partial desiccation during microscopic procedures. As the clathrin distribution was, however, not affected by this inevitable pretreatment, the interpretation of data presented in this study is not impaired. The rough appearance of plasma membrane after colocalization of clathrin and PtdIns(4,5)P_2 (Fig. 10) may indicate vesicle budding initiating membrane internalization and bulk-flow-endocytosis. While the dynamic distribution of fluorescent reporters for clathrin and PtdIns(4,5)P_2 were recorded over a longer period than two min, rapid structural changes in membrane organisation and plasmolysis make such images difficult to interpret. Occasional patterns of colocalized clathrin and the PtdIns(4,5)P_2-reporter in small punctate cytosolic particles may suggest internalized vesicles (data not shown), which have, however, not been imaged with reliable reproducibility. It must be noted that the time frame of lipid changes observed by biochemical analyses on whole plants grown in hydroponic culture cannot be

directly compared to the dynamics of clathrin relocalization in onion epidermal cells directly exposed to hypertonic medium.

In summary, the direct biochemical detection of unlabeled phospholipids in subcellular fractions of salt-stressed *Arabidopsis* leaves indicates that stress-induced increases in PtdIns4P and PtdIns(4,5)P_2 occur first at the plasma membrane and subsequently in CCVs. CCVs increase during hyperosmotic stress, possibly as one mechanism supporting bulk-flow endocytosis of membrane area during plasmolytic membrane rearrangement. Confocal imaging of fluorescent reporters transiently expressed in onion epidermal cells confirms stress-induced colocalization of PtdIns(4,5)P_2 with clathrin, the major coat protein of CCVs. The identification of the subcellular site of stress-induced PtdIns(4,5)P_2 increases in plant cells will serve as a basis for future investigations into the roles of PtdIns(4,5)P_2 in the formation of CCVs and in plant endocytosis.

Acknowledgements

We are indebted to Dr. Tamas Balla (National Institute for Child Health and Human Development, Rockville, MD, USA) for providing the HsPLCδ1-PH-domain-construct. We would also like to acknowledge gifts of the following antisera: anti-PMA2, Dr. Marc Boutry (Universite Catholique de Louvain, Louvain-la-Neuve, Belgium); anti-TGA2, Dr. Christiane Gatz (Göttingen University, Germany); anti-BiP, Dr. Alessando Vitale (Instituto Biosintesi Vegetali, Consiglio Nazionale delle Ricerche, Milan, Italy); anti-V-ATPase, Dr. Rafael Ratajczak (Institute of Botany, Technical University of Darmstadt, Darmstadt, Germany). We thank Dr. Ivo Feussner (Göttingen University, Germany) and Dr. Giselbert Hinz (Heidelberg University, Germany) for helpful discussion. We would also like to thank the following individuals at Göttingen University, Germany: Dr. Martin Fulda for plasmids; Dr. Andreas Wodarz and Dr. Michael Krahn for access to the confocal microscope and technical support, respectively; Susanne Mesters for expert plant culture. We gratefully acknowledge financial support through an Emmy Noether Grant from the German Research Foundation (DFG, to I.H.).

References

1 Balla, T. (2006) Phosphoinositide-derived messengers in endocrine signaling. J. Endocrinol. **188**, 135-153

2 Meijer, H. J. and Munnik, T. (2003) Phospholipid-based signaling in plants. Annu. Rev. Plant. Biol. **54**, 265-306

3 Stevenson, J. M., Perera, I. Y., Heilmann, I., Persson, S. and Boss, W. F. (2000) Inositol signaling and plant growth. Trends Plant Sci. **5**, 252-258

4 Milosevic, I., Sorensen, J. B., Lang, T., Krauss, M., Nagy, G., Haucke, V., Jahn, R. and Neher, E. (2005) Plasmalemmal phosphatidylinositol-4,5-bisphosphate level regulates the releasable vesicle pool size in chromaffin cells. J Neurosci **25**, 2557-2565

5 Vicogne, J., Vollenweider, D., Smith, J. R., Huang, P., Frohman, M. A. and Pessin, J. E. (2006) Asymmetric phospholipid distribution drives in vitro reconstituted SNARE-dependent membrane fusion. Proc. Natl. Acad. Sci. U. S. A. **103**, 14761-14766

6 Chernomordik, L. V. and Kozlov, M. M. (2005) Membrane hemifusion: crossing a chasm in two leaps. Cell **123**, 375-382

7 Cremona, O. and De Camilli, P. (2001) Phosphoinositides in membrane traffic at the synapse. J. Cell Sci. **114**, 1041-1052

8 Heilmann, I., Perera, I. Y., Gross, W. and Boss, W. F. (2001) Plasma membrane phosphatidylinositol 4,5-bisphosphate levels decrease with time in culture. Plant Physiol. **126**, 1507-1518

9 König, S., Mosblech, A. and Heilmann, I. (2007) Stress-inducible and constitutive phosphoinositide pools have distinct fatty acid patterns in *Arabidopsis thaliana*. FASEB J. **21**, 1958-1967

10 Perera, I. Y., Heilmann, I. and Boss, W. F. (1999) Transient and sustained increases in inositol 1,4,5-trisphosphate precede the differential growth response in gravistimulated maize pulvini. Proc. Natl. Acad. Sci. U. S. A. **96**, 5838-5843

11 Pical, C., Westergren, T., Dove, S. K., Larsson, C. and Sommarin, M. (1999) Salinity and hyperosmotic stress induce rapid increases in phosphatidylinositol 4,5-bisphosphate, diacylglycerol pyrophosphate, and phosphatidylcholine in Arabidopsis thaliana cells. J. Biol. Chem. **274**, 38232-38240

12 DeWald, D. B., Torabinejad, J., Jones, C. A., Shope, J. C., Cangelosi, A. R., Thompson, J. E., Prestwich, G. D. and Hama, H. (2001) Rapid accumulation of phosphatidylinositol 4,5-bisphosphate and inositol 1,4,5-trisphosphate correlates with calcium mobilization in salt-stressed Arabidopsis. Plant Physiol. **126**, 759-769

13 Heilmann, I., Perera, I. Y., Gross, W. and Boss, W. F. (1999) Changes in phosphoinositide metabolism with days in culture affect signal transduction pathways in *Galdieria sulphuraria*. Plant Physiol. **119**, 1331-1339

14 Doughman, R. L., Firestone, A. J. and Anderson, R. A. (2003) Phosphatidylinositol phosphate kinases put PI4,5P(2) in its place. J. Membr. Biol. **194**, 77-89

15 Mueller-Roeber, B. and Pical, C. (2002) Inositol phospholipid metabolism in Arabidopsis. Characterized and putative isoforms of inositol phospholipid kinase and phosphoinositide-specific phospholipase C. Plant Physiol. **130**, 22-46

16 Bunney, T. D., Watkins, P. A., Beven, A. F., Shaw, P. J., Hernandez, L. E., Lomonossoff, G. P., Shanks, M., Peart, J. and Drobak, B. K. (2000) Association of phosphatidylinositol 3-kinase with nuclear transcription sites in higher plants. Plant Cell **12**, 1679-1688

17 King, C. E., Stephens, L. R., Hawkins, P. T., Guy, G. R. and Michell, R. H. (1987) Multiple metabolic pools of phosphoinositides and phosphatidate in human erythrocytes incubated in a medium that permits rapid transmembrane exchange of phosphate. Biochem. J. **244**, 209-217

18 Staehelin, L. A. and Newcomb, E. H. (2000) Membrane structure and membranous organelles in Biochemistry and Molecular Biology of Plants (Buchanan, B. B., Gruissem, W. and Jones, R. L., eds.), pp. 2-50, American Society of Plant Physiologists, Rockville, MD

19 Einspahr, K. J., Maeda, M. and Thompson, G. A., Jr. (1988) Concurrent changes in Dunaliella salina ultrastructure and membrane phospholipid metabolism after hyperosmotic shock. J. Cell Biol. **107**, 529-538

20 Kinnunen, P. K. (2000) Lipid bilayers as osmotic response elements. Cell Physiol Biochem **10**, 243-250

21 Leshem, Y., Seri, L. and Levine, A. (2007) Induction of phosphatidylinositol 3-kinase-mediated endocytosis by salt stress leads to intracellular production of reactive oxygen species and salt tolerance. Plant J. **51**, 185-197

22 Randall, P. J. and Bouma, D. (1973) Zinc deficiency, carbonic anhydrase, and photosynthesis in leaves of spinach. Plant Physiol. **52**, 229-232

23 Gomord, V., Denmat, L. A., Fitchette-Laine, A. C., Satiat-Jeunemaitre, B., Hawes, C. and Faye, L. (1997) The C-terminal HDEL sequence is sufficient for retention of secretory proteins in the endoplasmic reticulum (ER) but promotes vacuolar targeting of proteins that escape the ER. Plant J. **11**, 313-325

24 Robinson, D. G. and Hinz, G. (2001) Organelle isolation in Plant cell biology: A practical approach (Satiat-Jeunemaitre, B. and Hawes, C., eds.), pp. 295-323, IRL Press, Oxford

25 Abe, S. and Davies, E. (1991) Isolation of F-actin from pea stems. Evidence from fluorescence microscopy. Protoplasma **163**, 51-61

26 Berkowitz, R. L. and Travis, R. L. (1981) Characterization and quantitation of concanavalin A binding by plasma membrane enriched fractions from soybean root. Plant Physiol. **68**, 1014-1019

27 Pierce, W. S. and Hendrix, D. L. (1979) Utilization of enzyme markers to determine the location of plasma membrane from *Pisum* epicotyls on sucrose gradients. Planta **146**, 161-169

28 Tarnowski, B. I., Spinale, F. G. and Nicholson, J. H. (1991) DAPI as a useful stain for nuclear quantitation. Biotech Histochem **66**, 297-302

29 Arnon, D. I. (1949) Copper enzymes in isolated chloroplasts. Polyphenoloxidase in *Beta vulgaris*. Plant Physiol. **24**, 1-15

30 Bradford, M. M. (1976) A rapid and sensitive method for the quantitation of microgram quantities of protein utilizing the principle of protein-dye binding. Anal. Biochem. **72**, 248-254

31 Laemmli, U. K. (1970) Cleavage of structural proteins during the assembly of the head of bacteriophage T4. Nature **227**, 680-5

32 Morsomme, P., Dambly, S., Maudoux, O. and Boutry, M. (1998) Single point mutations distributed in 10 soluble and membrane regions of the Nicotiana plumbaginifolia plasma membrane PMA2 H+-ATPase activate the enzyme and modify the structure of the C-terminal region. J. Biol. Chem. **273**, 34837-34842

33 Pedrazzini, E., Giovinazzo, G., Bielli, A., de Virgilio, M., Frigerio, L., Pesca, M., Faoro, F., Bollini, R., Ceriotti, A. and Vitale, A. (1997) Protein quality control along the route to the plant vacuole. Plant Cell **9**, 1869-1880

34 Liu, S. H., Wong, M. L., Craik, C. S. and Brodsky, F. M. (1995) Regulation of clathrin assembly and trimerization defined using recombinant triskelion hubs. Cell **83**, 257-267

35 Ratajczak, R., Feussner, I., Hause, B., Bohm, A., Parthier, B. and Wasternack, C. (1998) Alteration of V-type H^+-ATPase during methyljasmonate-induced senescence in barley (*Hordeum vulgare* L. cv. Salome). J. Plant Physiol. **152**, 199-206

36 Voller, A., Bidwell, D. E., Bartlett, A., Fleck, D. G., Perkins, M. and Oladehin, B. (1976) A microplate enzyme-immunoassay for toxoplasma antibody. J Clin Pathol **29**, 150-153

37 Cho, M. H., Chen, Q., Okpodu, C. M. and Boss, W. F. (1992) Separation and quantification of of [^{3}H]inositol phospholipids using thin-layer-chromatography and a computerized ^{3}H imaging scanner. LC-GC **10**, 464-468

38 Perera, I. Y., Davis, A. J., Galanopoulou, D., Im, Y. J. and Boss, W. F. (2005) Characterization and comparative analysis of Arabidopsis phosphatidylinositol phosphate 5-kinase 10 reveals differences in Arabidopsis and human phosphatidylinositol phosphate kinases. FEBS Lett. **579**, 3427-3432

39 Hartel, H., Dormann, P. and Benning, C. (2000) DGD1-independent biosynthesis of extraplastidic galactolipids after phosphate deprivation in Arabidopsis. Proc. Natl. Acad. Sci. U. S. A. **97**, 10649-10654

40 Christie, W. W. (2003) Thin-layer chromatography in Lipid analysis, vol. 15, pp. 142-152, The Oily Press, Bridgwater

41 König, S., Hoffmann, M., Mosblech, A. and Heilmann, I. (2008) Determination of content and fatty acid composition of unlabeled phosphoinositide species by thin layer chromatography and gas chromatography. Anal. Biochem., 197-201

42 Janke, C., Magiera, M. M., Rathfelder, N., Taxis, C., Reber, S., Maekawa, H., Moreno-Borchart, A., Doenges, G., Schwob, E., Schiebel, E. and Knop, M. (2004) A

versatile toolbox for PCR-based tagging of yeast genes: new fluorescent proteins, more markers and promoter substitution cassettes. Yeast **21**, 947-962

43 Varnai, P. and Balla, T. (1998) Visualization of phosphoinositides that bind pleckstrin homology domains: calcium- and agonist-induced dynamic changes and relationship to myo-[3H]inositol-labeled phosphoinositide pools. J. Cell Biol. **143**, 501-510

44 Dowd, P. E., Coursol, S., Skirpan, A. L., Kao, T. H. and Gilroy, S. (2006) Petunia phospholipase c1 is involved in pollen tube growth. Plant Cell **18**, 1438-1453

45 Hornung, E., Krueger, C., Pernstich, C., Gipmans, M., Porzel, A. and Feussner, I. (2005) Production of (10E,12Z)-conjugated linoleic acid in yeast and tobacco seeds. Biochim. Biophys. Acta **1738**, 105-114

46 Logemann, J., Schell, J. and Willmitzer, L. (1987) Improved method for the isolation of RNA from plant tissues. Anal. Biochem. **163**, 16-20

47 Klein, T. M., Harper, E. C., Svab, Z., Sanford, J. C., Fromm, M. E. and Maliga, P. (1988) Stable genetic transformation of intact Nicotiana cells by the particle bombardment process. Proc. Natl. Acad. Sci. U. S. A. **85**, 8502-8505

48 Harley, S. M. and Beevers, L. (1989) Coated vesicles are involved in the transport of storage proteins during seed development in *Pisum sativum* L. Plant Physiol. **91**, 674-678

49 Niggeweg, R., Thurow, C., Kegler, C. and Gatz, C. (2000) Tobacco transcription factor TGA2.2 is the main component of as-1-binding factor ASF-1 and is involved in salicylic acid- and auxin-inducible expression of as-1-containing target promoters. J. Biol. Chem. **275**, 19897-19905

50 Bunce, M. W., Bergendahl, K. and ANderson, R. A. (2006) Nuclear PI(4,5)P(2): a new place for an old signal. Biochem Biophys Acta **1761**, 560-569

51 Mellman, D. L., Gonzales, M. L., Song, C., Barlow, C. A., Wang, P., Kendziorski, C. and Anderson, R. A. (2008) A PtdIns4,5P2-regulated nuclear poly(A) polymerase controls expression of select mRNAs. Nature **451**, 1013-1017

52 Chen, C. N., Chu, C. C., Zentella, R., Pan, S. M. and Ho, T. H. (2002) AtHVA22 gene family in Arabidopsis: phylogenetic relationship, ABA and stress regulation, and tissue-specific expression. Plant Mol. Biol. **49**, 633-644

53 Takahashi, S., Katagiri, T., Yamaguchi-Shinozaki, K. and Shinozaki, K. (2000) An Arabidopsis gene encoding a Ca2+-binding protein is induced by abscisic acid during dehydration. Plant Cell Physiol. **41**, 898-903

54 Im, Y. J., Davis, A. J., Perera, I. Y., Johannes, E., Allen, N. S. and Boss, W. F. (2007) The N-terminal Membrane Occupation and Recognition Nexus Domain of Arabidopsis Phosphatidylinositol Phosphate Kinase 1 Regulates Enzyme Activity. J. Biol. Chem. **282**, 5443-5452

55 Blumental-Perry, A., Haney, C. J., Weixel, K. M., Watkins, S. C., Weisz, O. A. and Aridor, M. (2006) Phosphatidylinositol 4-phosphate formation at ER exit sites regulates ER export. Dev. Cell **11**, 671-682

56 Itoh, T., Ijuin, T. and Takenawa, T. (1998) A novel phosphatidylinositol-5-phosphate 4-kinase (phosphatidylinositol-phosphate kinase IIgamma) is phosphorylated in the endoplasmic reticulum in response to mitogenic signals. J. Biol. Chem. **273**, 20292-20299

57 Schleiff, E., Tien, R., Salomon, M. and Soll, J. (2001) Lipid composition of outer leaflet of chloroplast outer envelope determines topology of OEP7. Mol. Biol. Cell. **12**, 4090-4102

58 Bovet, L., Muller, M. O. and Siegenthaler, P. A. (2001) Three distinct lipid kinase activities are present in spinach chloroplast envelope membranes: phosphatidylinositol phosphorylation is sensitive to wortmannin and not dependent on chloroplast ATP. Biochem. Biophys. Res. Commun. **289**, 269-275

59 Justin, A. M., Kader, J. C. and Collin, S. (2002) Phosphatidylinositol synthesis and exchange of the inositol head are catalysed by the single phosphatidylinositol synthase 1 from Arabidopsis. Eur. J. Biochem. **269**, 2347-2352

60 Collin, S., Justin, A. M., Cantrel, C., Arondel, V. and Kader, J. C. (1999) Identification of AtPIS, a phosphatidylinositol synthase from Arabidopsis. Eur. J. Biochem. **262**, 652-658

61 Löfke, C., Ischebeck, T., König, S., Freitag, S. and Heilmann, I. (2008) Alternative metabolic fates of phosphatidylinositol produced by PI-synthase isoforms in Arabidopsis thaliana. Biochem. J. **413**, 115-124

62 Marza, E., Long, T., Saiardi, A., Sumakovic, M., Eimer, S., Hall, D. H. and Lesa, G. M. (2008) Polyunsaturated fatty acids influence synaptojanin localization to regulate synaptic vesicle recycling. Mol. Biol. Cell. **19**, 833-842

63 Jost, M., Simpson, F., Kavran, J. M., Lemmon, M. A. and Schmid, S. L. (1998) Phosphatidylinositol-4,5-bisphosphate is required for endocytic coated vesicle formation. Curr. Biol. **8**, 1399-1402

64 van Leeuwen, W., Vermeer, J. E., Gadella, T. W., Jr. and Munnik, T. (2007) Visualization of phosphatidylinositol 4,5-bisphosphate in the plasma membrane of suspension-cultured tobacco BY-2 cells and whole Arabidopsis seedlings. Plant J. **52**, 1014-1026

Figure Legends

Figure 1. Enrichment of subcellular fractions from *Arabidopsis* rosette leaves. Major membrane fractions were enriched from leaf material of six-week-old *Arabidopsis* plants, and the lipid composition of the individual fractions was tested by thin-layer-chromatography. Lipid extracts were subjected to chromatography and lipids visualized by charring. Lipids were identified according to comigration with authentic standards. DGDG, digalactosyldiacylglycerol; diPtdGro, cardiolipin; MGDG, monogalactosyldiacylglycerol; n.i. not identified lipid; NL, neutral lipids; PtdGro, phosphatidylglycerol; PtdEtn, phosphatidylethanolamine; PtdOH, phosphatidic acid; PtdCho, phosphatidylcholine; SG, sterol glycosides

Figure 2. Unlabeled PtdIns(4,5)P_2 can be detected in plant extracts. The migration of PtdIns(4,5)P_2 was tested in relation to more abundant phospholipids. A, TLC-separation of leaf extracts using a developing solvent containing $CHCl_3$:CH_3OH:H_2O:acetic acid at volume ratios of 10:10:3:1. Lipid extracts from non-stressed rosette leaves were used without (I) or with addition (II) of a spiking amount of 0.5 µg of 1-stearoyl, 2-arachidonoyl-PtdIns(4,5)P_2 (Avanti). M, Authentic PtdIns(4,5)P_2 standard (Avanti). B, PtdIns(4,5)P_2 was isolated from TLC-plates according to [41], and fatty acids associated with the isolated lipids analyzed by GC. Solid line, PtdIns(4,5)P_2 from plant extract; dotted line, PtdIns(4,5)P_2 from plant extract spiked with exogenous PtdIns(4,5)P_2. Peak identities are indicated; 16:0, palmitic acid; 18:0, stearic acid; 18:1, oleic acid; 18:2, linoleic acid; 18:3, linolenic acid; 20:4, arachidonic acid; i. s., pentadecanoic acid internal standard

Figure 3. Fatty acid composition of phospholipids in enriched subcellular fractions. Lipids were extracted from enriched subcellular fractions, isolated, and their associated fatty acids determined. Fractions analyzed were plasma membranes (PM), an F-actin enriched fraction (F-A), nuclei (N), endoplasmic reticulum (ER), and clathrin-coated vesicles (CCV). Fatty acids associated with different phospholipids isolated from the individual fractions are indicated by bars with different patterns; the identity of the fatty acids is also indicated at the bottom. 16:0, palmitic acid; 18:0, stearic acid; 18:1, oleic acid; 18:2, linoleic acid; 18:3, linolenic acid. PtdCho, phosphatidylcholine; PtdEtn, phosphatidylethanolamine; PtdIns, phosphatidylinositol; PtdIns4P, phosphatidylinositol-4-phosphate; PtdIns(4,5)P_2, phosphatidylinositol-4,5-bisphosphate. Data are given as mol% of total fatty acids and represent the mean ± SD of three to seven independent experiments.

Figure 4. Stress-induced dynamic changes in PIs in plasma membranes. Plants grown in hydroponic culture were subjected to hyperosmotic stress, and leaf material was collected after different time periods of stimulation. Lipids were extracted from enriched plasma membrane (PM) and endomembrane fractions (EM), PIs isolated, and their associated fatty acids determined. Bars represent the total amounts of fatty acids associated with individual lipids; the bar segments indicate the contribution of individual fatty acids: white, 16:0; diamonds, 18:0; grey, 18:1Δ^9; striped, 18:2$\Delta^{9,12}$; black, 18:3$\Delta^{9,12,15}$. PtdIns, phosphatidylinositol; PtdIns4P, phosphatidylinositol-4-phosphate; PtdIns(4,5)P_2, phosphatidylinositol-4,5-bisphosphate. Data are given as pmol g^{-1} fresh weight and represent the mean ± SD of three independent experiments.

Figure 5. Stress-induced dynamic changes in PIs in different endomembranes. Plants grown in hydroponic culture were subjected to hyperosmotic stress, and leaf material was collected after different time periods of stimulation. Lipids were extracted from fractions enriched for endoplasmic reticulum (ER), nuclei, or plastids, as indicated, and their associated

fatty acids determined. Bars represent the total amounts of fatty acids associated with individual lipids; the bar segments indicate the contribution of individual fatty acids: white, 16:0; diamonds, 18:0; grey, 18:1Δ^{9}; striped, 18:2$\Delta^{9,12}$; black, 18:3$\Delta^{9,12,15}$. PtdIns, phosphatidylinositol; PtdIns4P, phosphatidylinositol-4-phosphate; PtdIns(4,5)P_2, phosphatidylinositol-4,5-bisphosphate. Data are given as pmol g^{-1} fresh weight and represent the mean ± SD of three to five independent experiments.

Figure 6. Unimpaired transcript induction in plants exposed to salt stress. Plants grown in hydroponic culture were subjected to hyperosmotic stress, leaf material was collected after different time periods of stimulation, and transcript levels for stress inducible genes were determined by Northern-blot analysis. Transcripts detected included *HVA* (high voltage activated) and *RD20* (responsive to desiccation). The *ACT8* transcript (actin) was tested as a control. The data presented are from a representative experiment; the experiment was repeated twice with similar results.

Figure 7. Increased formation of clathrin-coated vesicles with hyperosmotic stress. Plants grown in hydroponic culture were subjected to hyperosmotic stress, leaf material was collected after different time periods of stimulation, and CCVs were enriched. A, Protein extracts from 30 g of leaf tissue were separated by SDS-PAGE, and proteins stained with Coomassie blue (left panel). The overall staining intensity of CCV-associated proteins from non-stimulated plants and from plants stimulated for 60 min were determined, as indicated (right panel). Protein patterns shown (left panel) are from a representative experiments. The experiment was repeated twice with similar results; the quantification (right panel) indicates the mean of three experiments ± SD. B, Lipids were extracted from CCV-enriched fractions, and their associated fatty acids determined. Bars represent the total amounts of fatty acids associated with individual lipids; the bar segments indicate the contribution of individual fatty acids: white, 16:0; diamonds, 18:0; grey, 18:1Δ^{9}; striped, 18:2$\Delta^{9,12}$; black, 18:3$\Delta^{9,12,15}$. PtdIns, phosphatidylinositol; PtdIns4P, phosphatidylinositol-4-phosphate; PtdIns(4,5)P_2, phosphatidylinositol-4,5-bisphosphate. Data are given as pmol g^{-1} fresh weight and represent the mean ± SD of three independent experiments.

Figure 8. Stress-induced increases in PtdIns(4,5)P_2 associated with clathrin-coated vesicles. Plants grown in hydroponic culture were subjected to hyperosmotic stress, and leaf material was collected after different time periods of stimulation. A, Lipids were extracted from fractions enriched for CCVs and their associated fatty acids determined. Bars represent the total amounts of fatty acids associated with individual lipids; the bar segments indicate the contribution of individual fatty acids: white, 16:0; diamonds, 18:0; grey, 18:1Δ^{9}; striped, 18:2$\Delta^{9,12}$; black, 18:3$\Delta^{9,12,15}$. PtdIns, phosphatidylinositol; PtdIns4P, phosphatidylinositol-4-phosphate; PtdIns(4,5)P_2, phosphatidylinositol-4,5-bisphosphate. Data are given as pmol g^{-1} fresh weight and represent the mean ± SD of four independent experiments. B, The mass ratios of PtdIns(4,5)P_2/PtdCho for each time point were calculated based on data in A and Figure 7 B. An increased ratio indicates increased association of PtdIns(4,5)P_2 with CCVs.

Figure 9. Stress-induced colocalization of PtdIns(4,5)P_2 with clathrin in onion epidermal cells. Onion epidermal cells were transiently cotransformed with EYFP-tagged clathrin and with a RedStar-tagged reporter for PtdIns(4,5)P_2 (RedStar-PLCδ1-PH). The fluorescence distribution of bright field (top), EYFP (green) and RedStar (red) was synchronously and continuously monitored by confocal microscopy in cells subjected to hyperosmotic stress. Yellow color in the bottom panels indicates colocalization. Time points over the first two minutes of stimulation are depicted. A, Bright field; B, RedStar-PLCδ1-PH; C, EYFP-clathrin; D, Merged image. V, vacuole; T, tonoplast; C, cytosol; PM, plasma membrane. Images shown

are from a representative experiment; the transformation experiment was repeated twice with similar results. Bars, 20 μm

Figure 10. Stress-induced changes in plasma membrane appearance. The fluorescence distribution of bright field (top), EYFP (green) and RedStar (red) was synchronously and continuously monitored by confocal microscopy in cells subjected to hyperosmotic stress. Plasma membrane areas indicated in Figure 9 were scanned at higher magnification to resolve the distribution of PtdIns(4,5)P_2 and clathrin in relation to rearrangements of the plasma membrane during stress-exposure. Time points chosen reflect the non-stimulated situation (0) and the situation 60 s after stimulation. Images shown are from a representative experiment; the transformation experiment was repeated twice with similar results. Bars, 5 μm

Biochemical Journal Immediate Publication. Published on 22 Aug 2008 as manuscript BJ20081306

Figure 1

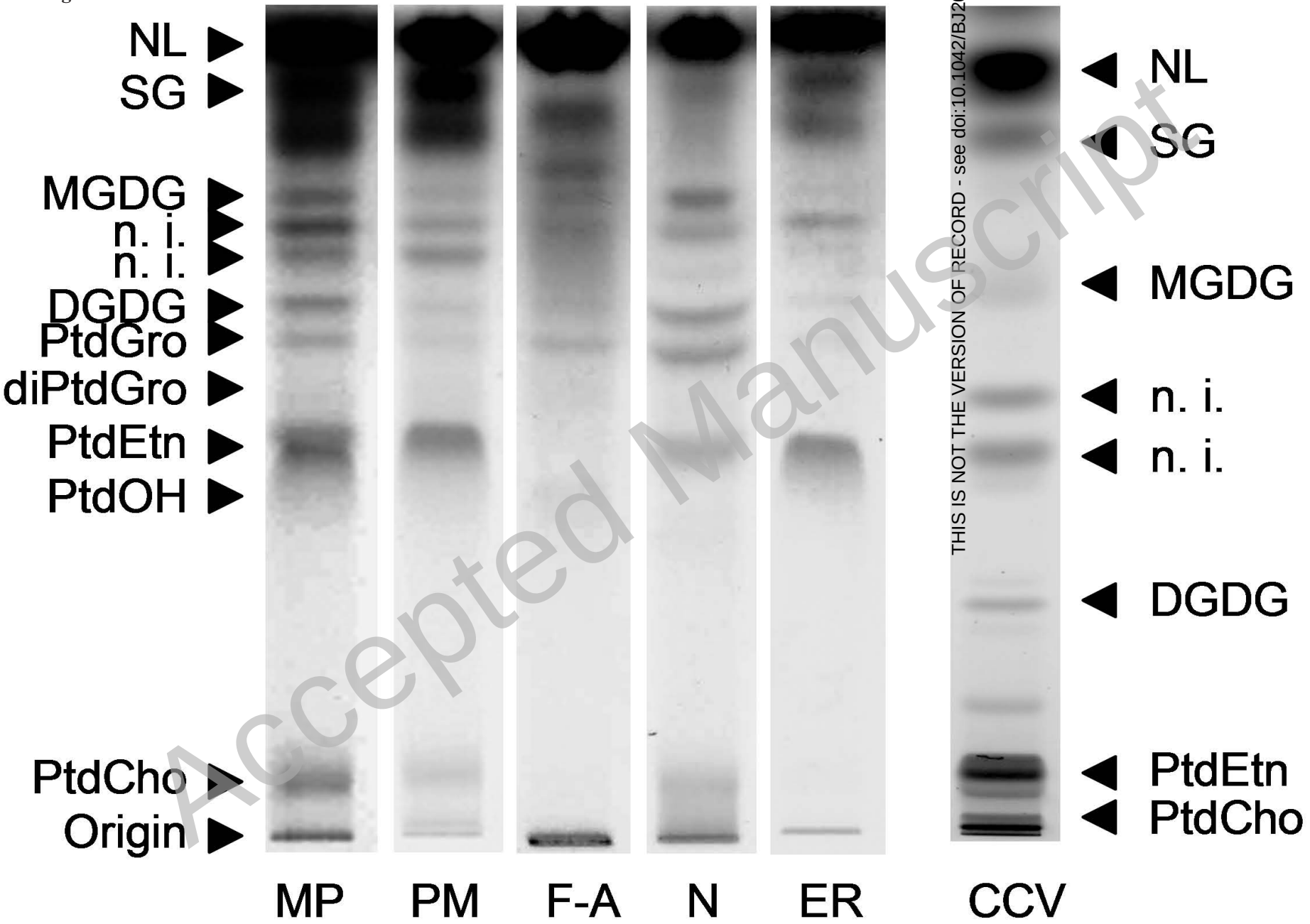

Figure 2

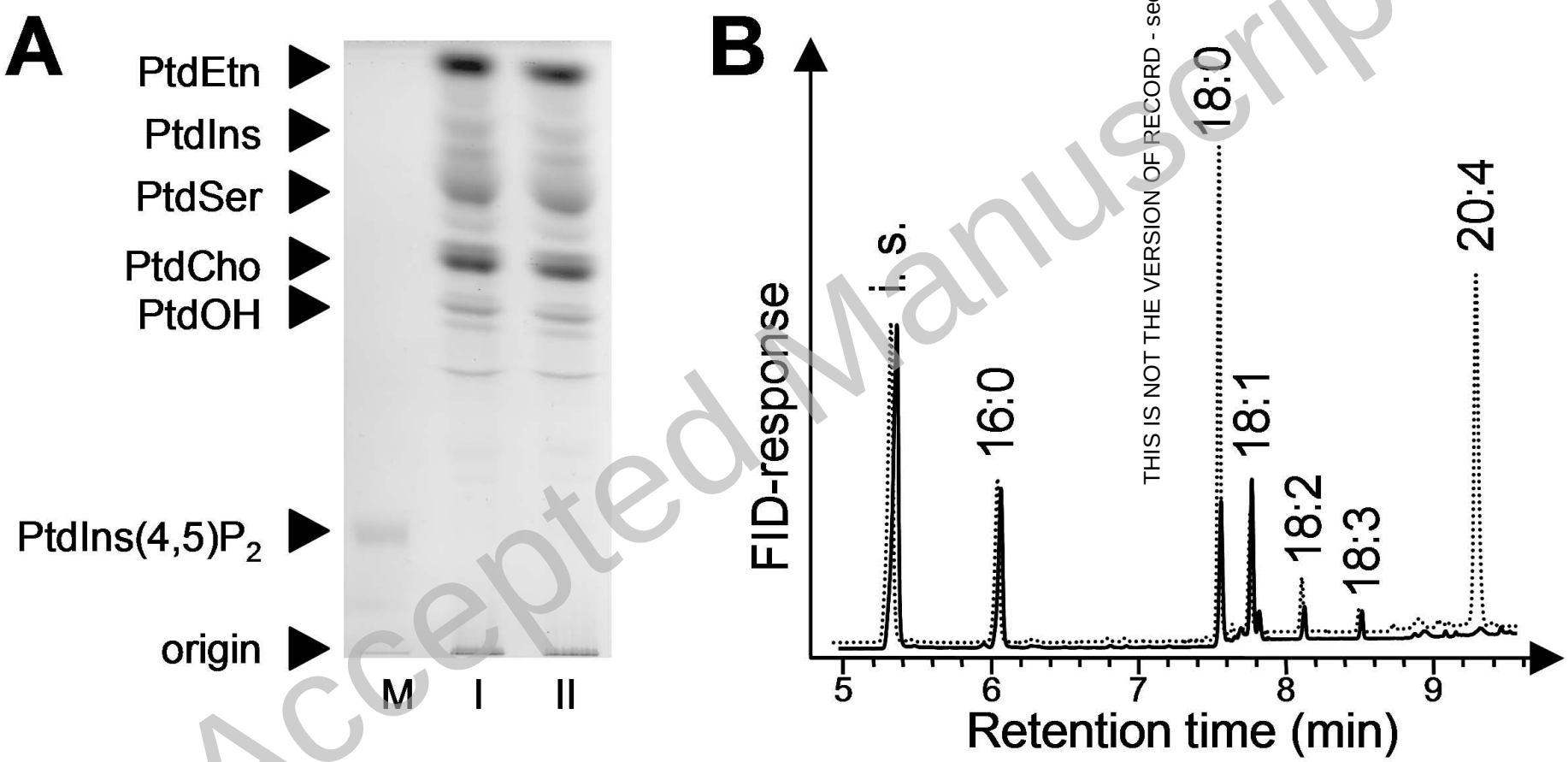

Biochemical Journal Immediate Publication. Published on 22 Aug 2008 as manuscript BJ20081306

Figure 3

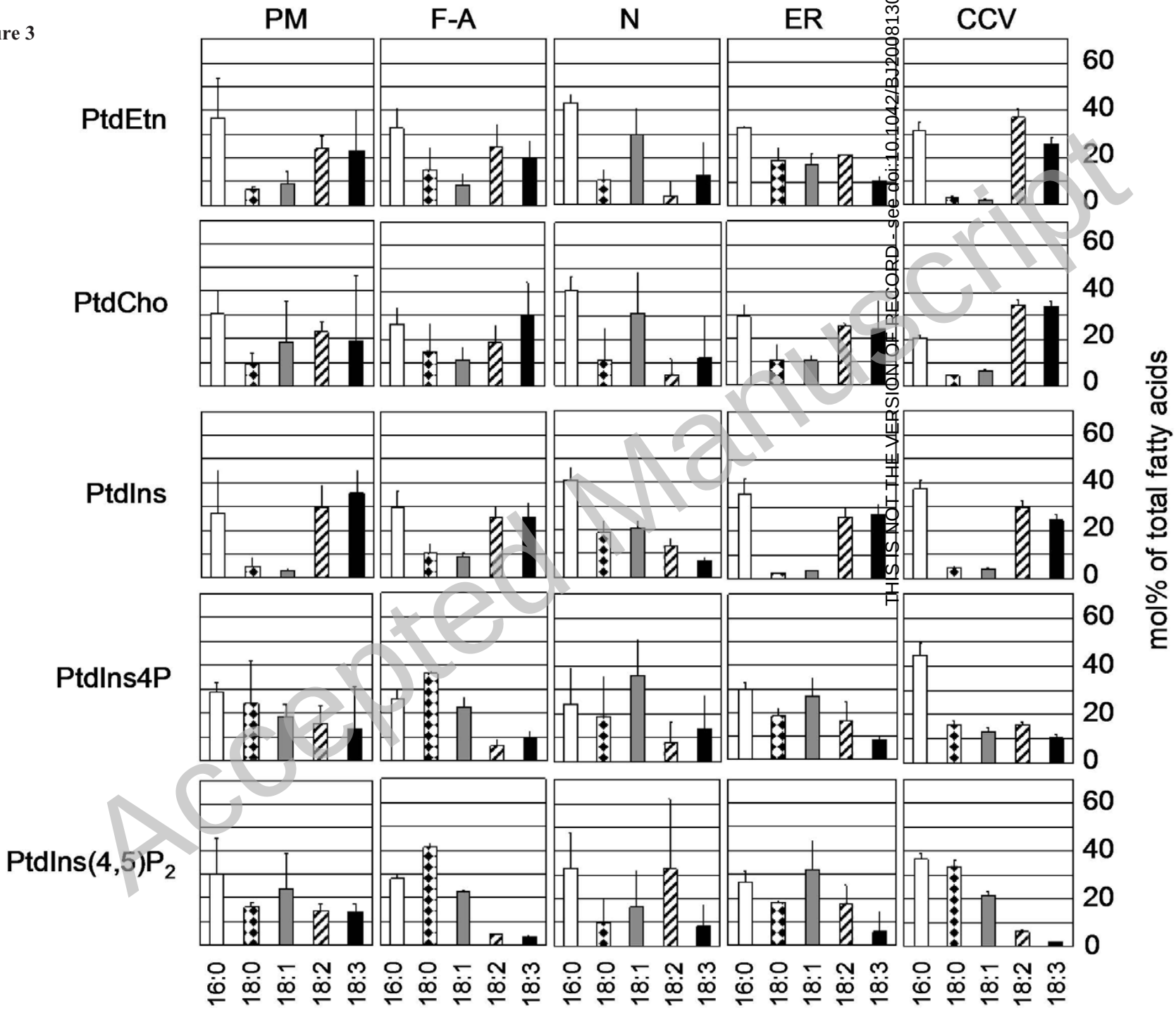

Figure 4

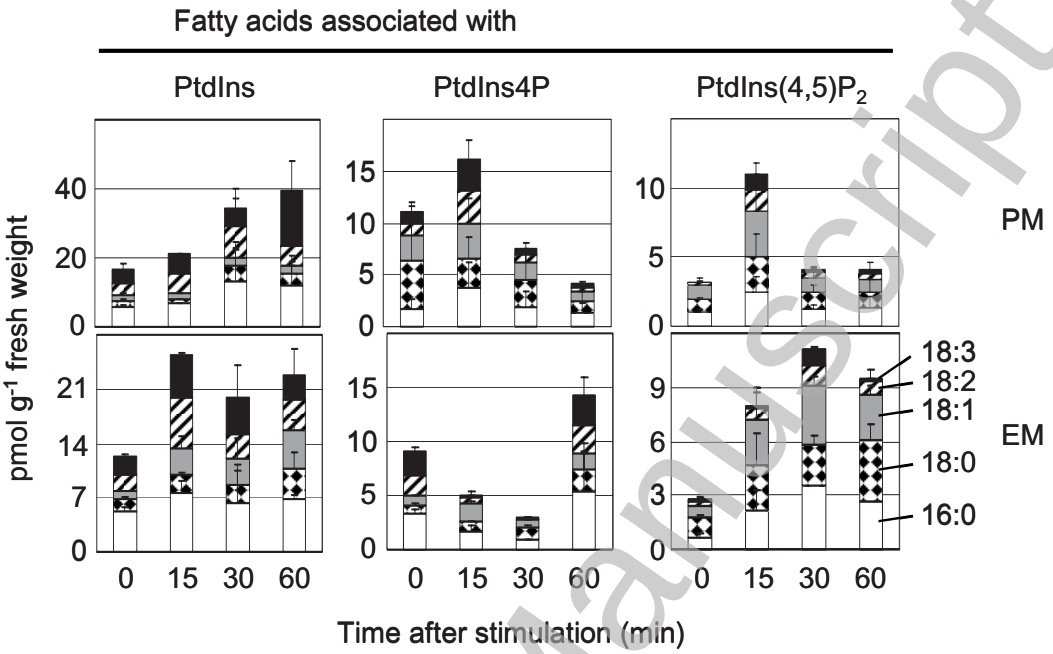

Figure 5

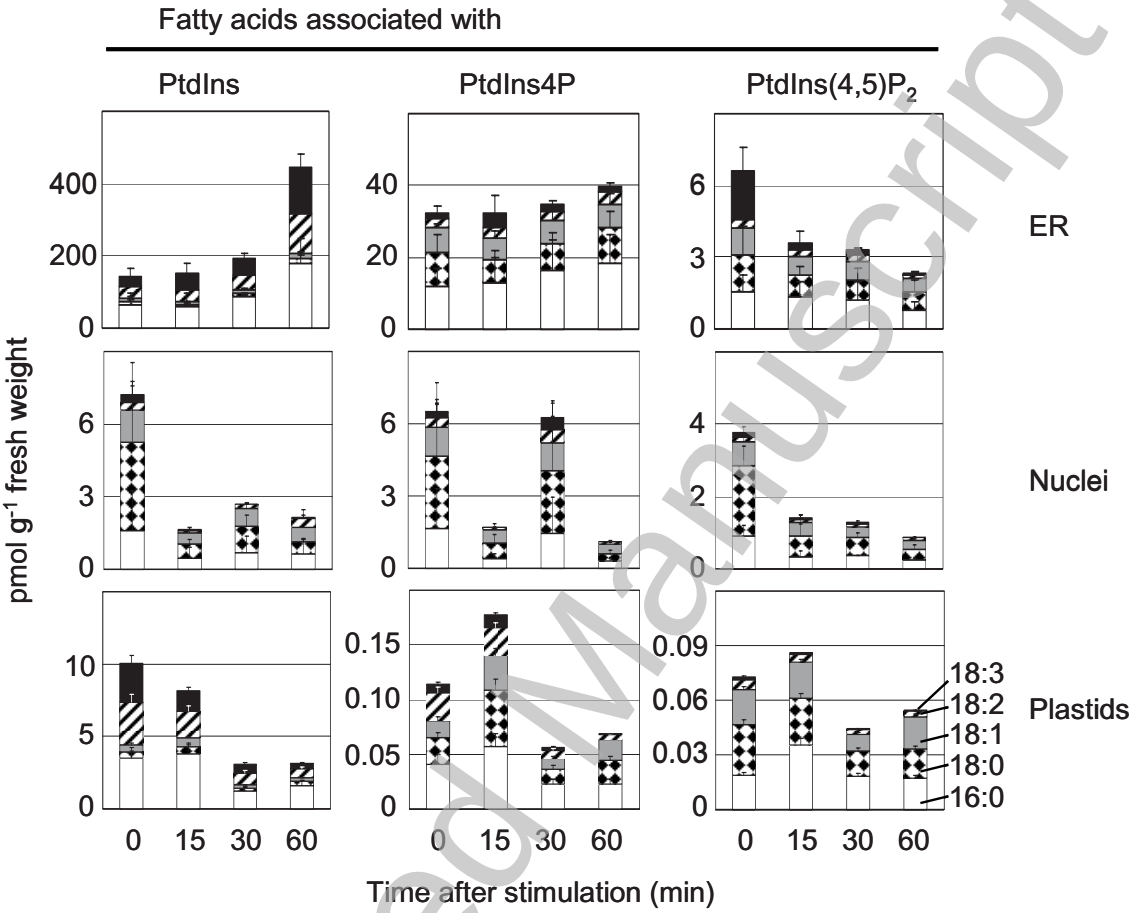

Biochemical Journal Immediate Publication. Published on 22 Aug 2008 as manuscript BJ20081306

Figure 6

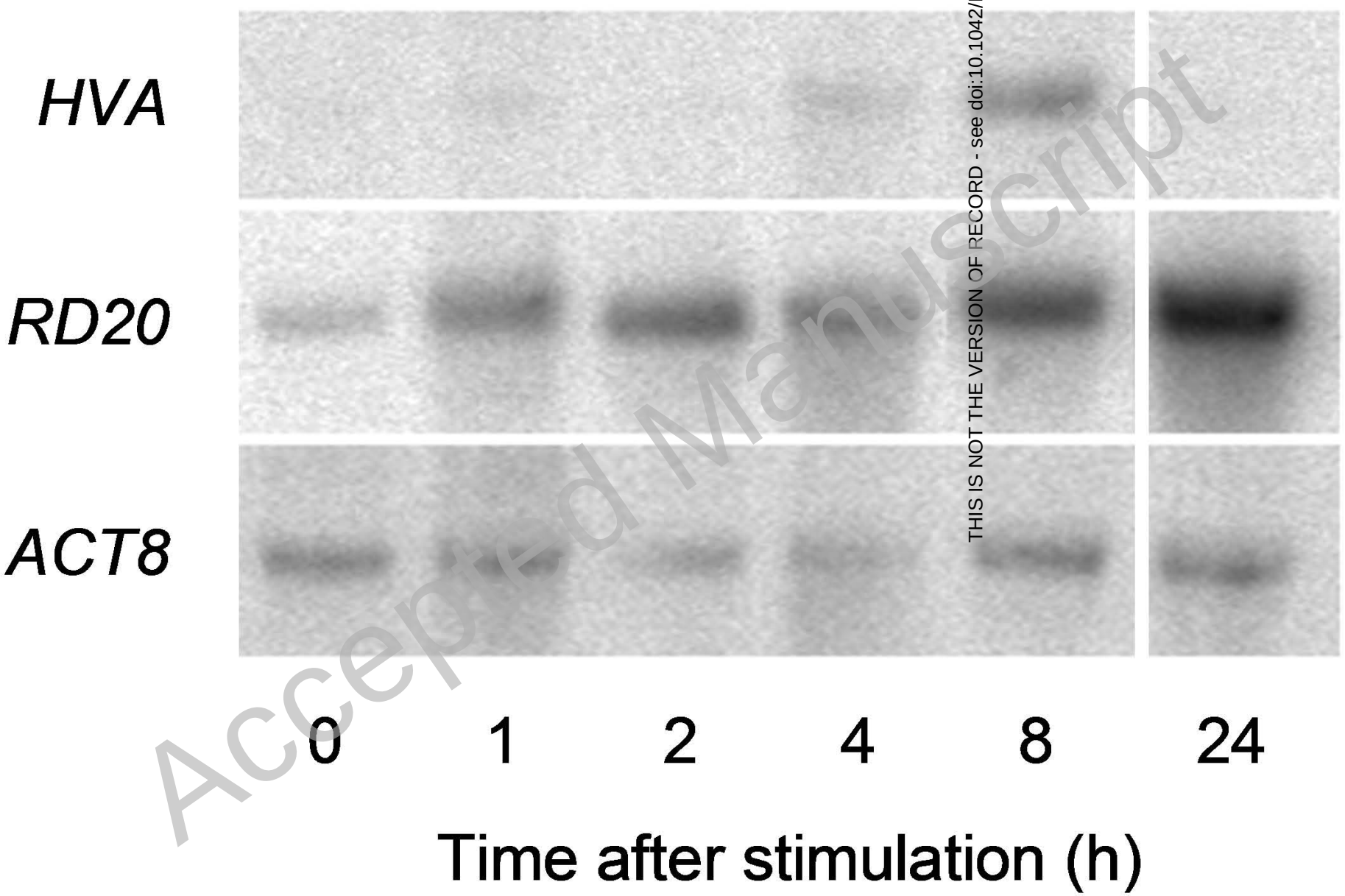

Figure 7

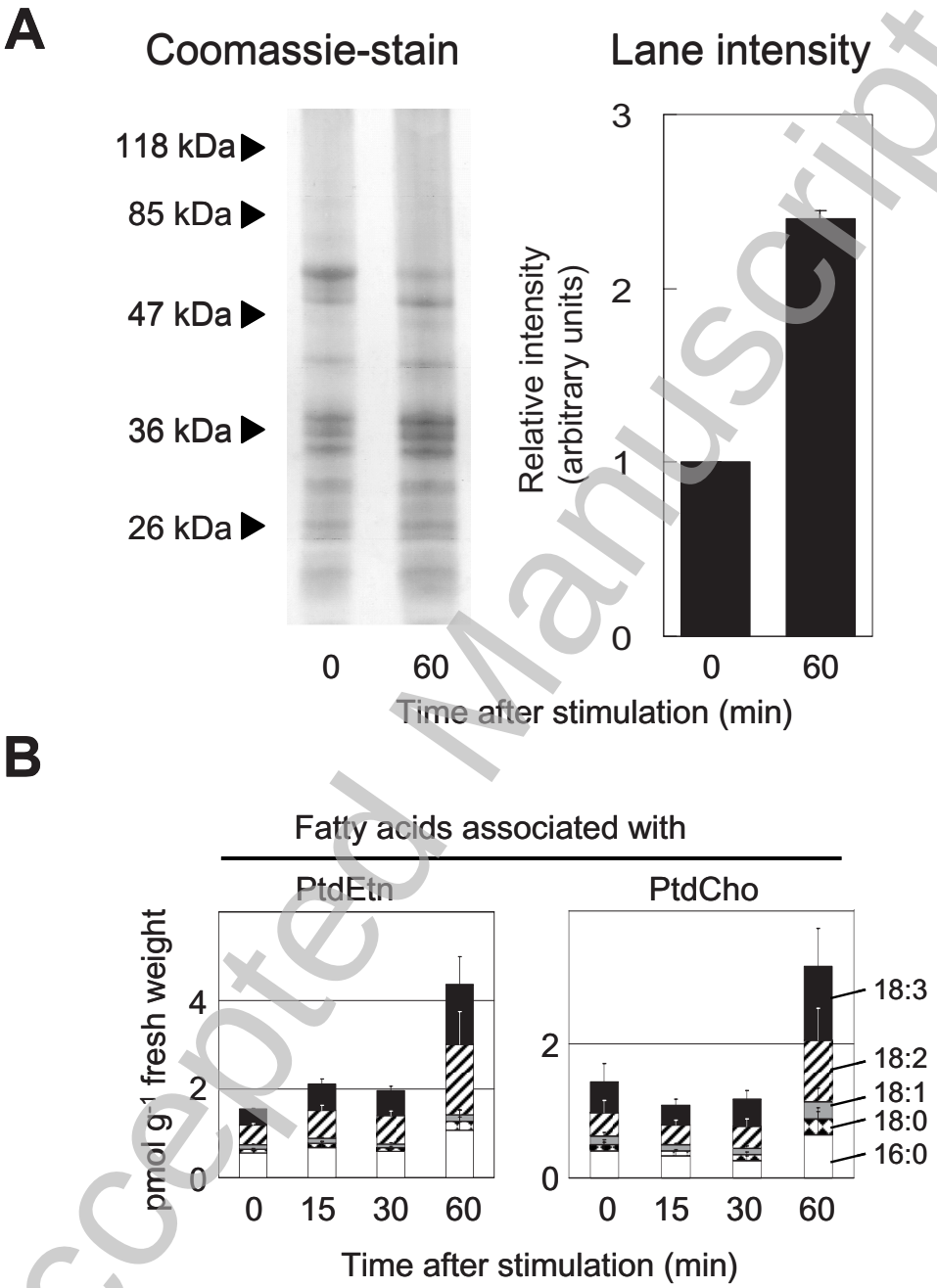

Figure 8

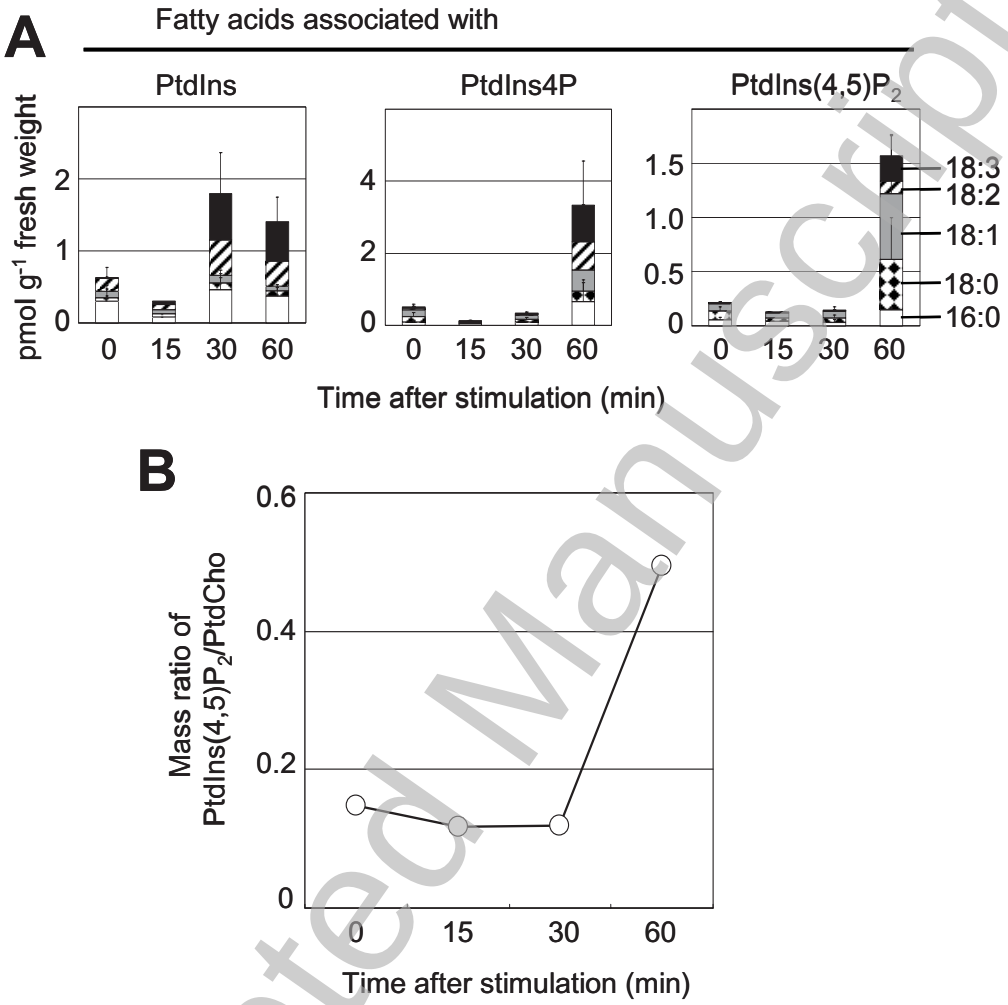

Biochemical Journal Immediate Publication. Published on 22 Aug 2008 as manuscript BJ20081306

See doi:10.1042/BJ20081306

Figure 9

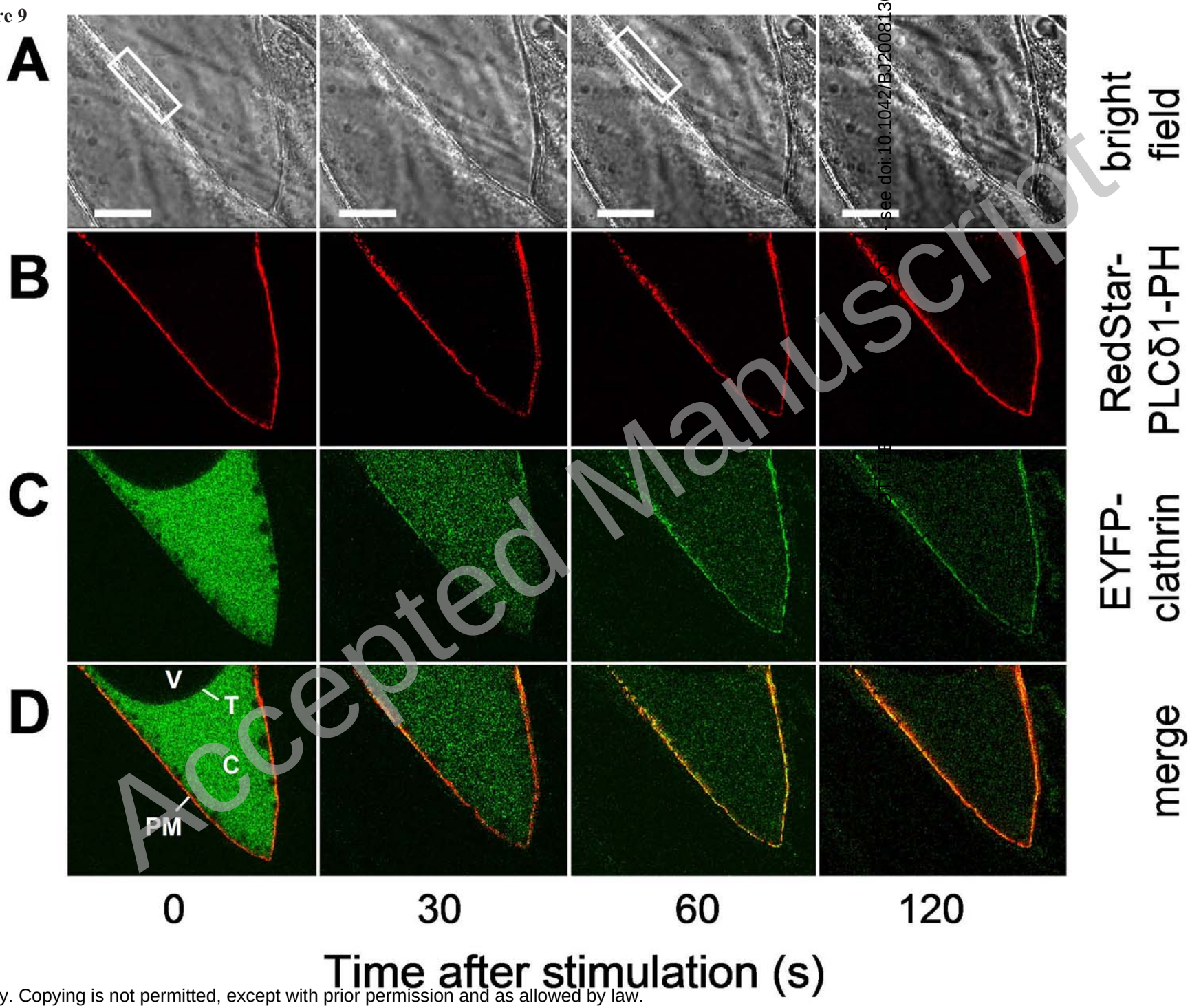

Biochemical Journal Immediate Publication. Published on 22 Aug 2008 as manuscript BJ20081306

Figure 10